Journal of Theoretical Biology 402 (2016) 9–17

Contents lists available at ScienceDirect

Journal of Theoretical Biology

journal homepage: www.elsevier.com/locate/yjtbi

The mutation–drift balance in spatially structured populations

David M. Schneider, Ayana B. Martins, Marcus A.M. de Aguiar *

Instituto de Física 'Gleb Wataghin', Universidade Estadual de Campinas, Unicamp 13083-970, Campinas, SP, Brazil

HIGHLIGHTS

- We model population structure using networks of constant degree k.
- Evolution follows a Moran process and is mapped into the voter model.
- If k is small, substantially smaller mutation rates are enough to overcome drift.
- The critical k for overcoming drift increases as a power law with population size.
- The stationary distribution becomes tri-modal at this mutation threshold.

GRAPHICAL ABSTRACT

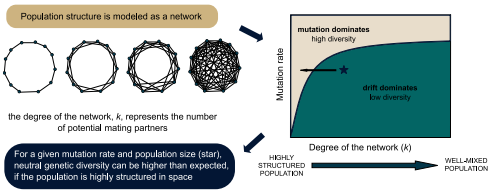

ARTICLE INFO

Article history:
Received 2 October 2015
Received in revised form
22 February 2016
Accepted 18 April 2016
Available online 27 April 2016

Keywords:
Allele distribution
Mutation threshold
Networks
Moran model

ABSTRACT

In finite populations the action of neutral mutations is balanced by genetic drift, leading to a stationary distribution of alleles that displays a transition between two different behaviors. For small mutation rates most individuals will carry the same allele at equilibrium, whereas for high mutation rates of the alleles will be randomly distributed with frequencies close to one half for a biallelic gene. For well-mixed haploid populations the mutation threshold is $\mu_c = 1/2N$, where N is the population size. In this paper we study how spatial structure affects this mutation threshold. Specifically, we study the stationary allele distribution for populations placed on regular networks where connected nodes represent potential mating partners. We show that the mutation threshold is sensitive to spatial structure only if the number of potential mates is very small. In this limit, the mutation threshold decreases substantially, increasing the diversity of the population at considerably low mutation rates. Defining k_c as the degree of the network for which the mutation threshold drops to half of its value in well-mixed populations we show that k_c grows slowly as a function of the population size, following a power law. Our calculations and simulations are based on the Moran model and on a mapping between the Moran model with mutations and the voter model with opinion makers.

1. Introduction

Despite the ongoing debate over the relative importance of randomness and environmental selection in determining the properties of organisms during evolution, stochastic processes are certainly an inherent property of living populations. In particular, random variation in the outcome of different life-history events collectively result in what is often summarized in the concept of "random genetic drift" (Lenormand et al., 2009). Although its influence in large populations may be weak when compared to selection, its role can be decisive in the process of fixation of rare alleles and cannot be neglected in small populations.

In population genetics, mutation and genetic drift are two inescapable sources of stochasticity with opposing effects regarding the maintenance of variation in the population. In the case of a single biallelic locus under reversible mutation, the dynamics of allele frequencies can be calculated in the limit of large and well-mixed (panmictic) populations. The equilibrium distribution converges to a Beta distribution that resembles a Gaussian for high

* Corresponding author.

http://dx.doi.org/10.1016/j.jtbi.2016.04.024
0022-5193/

mutation rates and a U-shaped curve for small mutation rates (Crow and Kimura, 1970; Gillespie, 2004). These two regimes reflect the relative importance of each evolutionary force in the dynamics. For a haploid population of size N and mutation rate μ, drift dominates whenever $2\mu N \ll 1$. In this regime, one of the alleles becomes nearly fixed. For $2\mu N \gg 1$, on the other hand, mutation dominates over drift and both alleles evolve to nearly equal frequencies, maximizing genetic diversity. The transition occurs at a well defined threshold, $\mu_c = 1/2N$, where the equilibrium distribution of allelic frequencies becomes uniform. The dynamics can also be computed with the help of hypergeometric functions. The exact dynamics for populations of arbitrary size was only recently computed (Chinellato et al., 2015). When several loci and multiple alleles are taken into account the equilibrium condition gives the expected genetic diversity under neutrality, which may be taken as a null model for testing the effects of other evolutionary forces (Crow and Kimura, 1970).

The consequences of random genetic drift were first worked out by Wright and Fisher using a formulation currently known as the Wright–Fisher process (Gillespie, 2004). From these early results, it became apparent how drift could generate genetic differentiation between subdivided populations. Subsequently, the study of genetic drift and population structure became entwined. Contrary to early results that suggested that population structure could have little effect on evolutionary dynamics (reviewed in Ewens, 2004), it has been shown that the dynamics of allele frequencies is sensitive to the spatial distribution of individuals in a population. Specifically, the roles of mutation, selection and drift can be affected by the geographical structure, and quantities like fixation probability, time to fixation and allele distribution can differ significantly from those derived for panmictic populations (see for example Whitlock, 2003; Lieberman et al., 2005; Patwa and Wahl, 2008; Constable and McKane, 2014; Allen, 2015).

Following Wright's (1931) classic island model, spatial structure has often been implemented by assuming that the population is divided into islands of arbitrary sizes, or demes, which are connected by migration. The connections can be seen as network links, which can connect all demes between each other to form a complete graph, or acquire more complex structures (see Constable and McKane, 2014 for a recent overview on island models). More recently, evolutionary graph theory has been introduced as a framework that could provide a more general account of any arbitrary population structure (Lieberman et al., 2005). In this case, the individuals themselves are placed in the nodes of a network and links represent interactions between pairs of individuals (Lieberman et al., 2005; Dick and Whigham, 2005; Gordo and Campos, 2006; Whigham and Dick, 2007; Tarnita et al., 2009; Voorhees, 2013; Monk et al., 2014; Allen, 2015). The main focus of these studies has been how population structure may affect the drift-selection balance (Lieberman et al., 2005; Gordo and Campos, 2006; Whigham and Dick, 2007; Tarnita et al., 2009; Voorhees, 2013; Monk et al., 2014) and/or the fate of a single mutation (Lieberman et al., 2005; Dick and Whigham, 2005; Whigham and Dick, 2007; Voorhees, 2013; Monk et al., 2014; Allen, 2015). Not much attention has been given to the balance between drift and mutation and the properties of the stationary allele distribution that arises in such process.

The aim of this paper is to quantify the effects of spatial structure on the genetic variability and allele distribution under the mutation-drift balance. We study a single biallelic gene in a population of haploid individuals within the framework of a Moran process on a network, for which exact results are known for panmictic populations. In this model, an individual chosen at random is substituted by a copy of another randomly chosen individual. Although the model has been proposed and studied in the context of population genetics (Watterson, 1961; Cannings, 1974; Gladstien, 1978; Ewens, 2004), the process has found applications in other areas, such as the spreading of cancer (Durrett and Moseley, 2015) and the evolution of altruism (Débarre et al., 2014). We also use results from the *voter model*, a closely related process developed in connection with the social sciences (Mobilia et al., 2007; Harmon et al., 2015; Liggett, 2012; Yildiz et al., 2013; Chinellato et al., 2015) with applications in physics (Mobilia, 2003; Mobilia et al., 2007). In this case, individuals have to choose between two candidates in an election and their opinions are influenced by other voters and external *opinion makers*. It has been recognized that the Moran model bears a close resemblance to the voter model. The connection was proven for well-mixed populations with mutations (de Aguiar and Bar-Yam, 2011) and for regular networks without mutations (Durrett and Moseley, 2015). In particular, the phase transition from disordered to ordered states exhibited by the voter model when the number of opinion makers for each candidate is exactly one is mapped into the critical mutation rate $\mu_c = 1/2N$ of the Moran model.

Our main interest is to understand how the threshold changes for spatially structured populations. To that purpose, we place the N individuals on a regular network, where each successive node is connected to its k nearest neighbors, so that all nodes have the same degree k. We study the configurations ranging from $k = N - 1$ to $k=2$, which correspond to the extremes of panmictic to ring populations (in which individuals are in contact only with their two nearest neighbors). In the first place, we provide a connection between the Moran and voter models for networks of arbitrary topologies. We show that a direct equivalence exists for regular networks, where every node has the same degree k. Using approximate solutions that are available for the voter model we show that the equilibrium distributions of the Moran model should not be sensitive to k, *i.e.* that the genetic distribution should be independent of the population's spatial structure. However, analytical results for a small network and numerical simulations show that these approximations break down if k is small. For sufficiently low values of k the critical mutation, above which mutation dominates over drift, decreases substantially. As a consequence, populations that display marked spatial structure can have much higher diversity than expected for well-mixed ones. We define a critical value k_c as the degree for which the mutation threshold drops to half of its panmictic value and show that k_c grows slowly as a function of N following a power law.

2. The voter model with opinion makers on networks

The voter model consists of a set of individuals who must choose between two candidates (Liggett, 2012). Their opinion can be influenced by their friends and by opinion makers, such as journalists or politicians, whose power of persuasion toward one of the candidates extends over the entire population. The opinion makers are modeled by additional (external) nodes whose states are fixed and that reach all voters equally, acting as a perturbation to the intrinsic dynamics.

The population has N voters placed on the nodes of a network and connected according to a specified adjacency matrix A, defined by $A_{ij} = 1$ if the nodes i and j are connected and $A_{ij} = 0$ otherwise. Each node has an internal state which can take the values 0 or 1, indicating the intention of vote toward candidate 0 or candidate 1, respectively. The nodes are also connected to N_0 nodes whose states are fixed at 0 and to N_1 nodes whose states are fixed at 1, representing the opinion makers. In what follows we will refer as *free nodes* to those representing the set of voters and as *frozen nodes* to those referring to opinion makers. The free nodes can change their internal state by adopting the opinion of a connected friend or that of an opinion maker as specified below.

In order to study the dynamics of the system we introduce the following notation: we designate as $x = (x_1, x_2, \ldots, x_i, \ldots, x_N)$ to the microscopic state of the network, in which the state of each node is specified. In addition, we define the auxiliary microscopic state $x^i = (x_1, x_2, \ldots, 1 - x_i, \ldots, x_N)$, corresponding to the state that differs from x only at node i.

The network dynamics is as follows: at each time step a free node is chosen at random. This node can maintain its state with probability p, or copy the state of an other node with probability $1 - p$. In the case it copies a state of another node, the latter is randomly chosen between the neighbors (specified by the adjacency matrix) and the frozen nodes. Because only one node is updated at each time step, we can write the probability of finding the network in state x at time $t + 1$ as follows:

$$P_{t+1}(x) = pP_t(x) + (1-p)\frac{1}{N}P_t(x)\sum_{i=1}^{N} T(x_i \to x_i) + (1-p)\sum_{i=1}^{N}\frac{1}{N}P_t(x^i)T(x_i^i \to x_i). \quad (1)$$

The first two terms in Eq. (1) take into account the probability of having the network in the state x at time t, and correspond to the cases in which (i) the selected node does not change its state or (ii) the selected node copies the state of a neighbor whose state is identical to its own state. The last term represents the probability of having the network in any of the states x^i at time t, to select node i to be updated and to choose a neighbor whose state is precisely x_i (so that the state x is recovered at time $t + 1$). Detailed calculations of the transition probabilities $T(x_i \to x_i)$ and $T(x_i^i \to x_i)$ can be found in Appendix A. Introducing the explicit expressions, Eq. (1) reads

$$P_{t+1}(x) = P_t(x) + \frac{(1-p)}{N}P_t(x)\sum_{i=1}^{N}\frac{1}{k_i + N_0 + N_1}\left[\sum_{j=1}^{N}A_{ij}|1 - x_i - x_j| - k_i - (1-x_i)N_1 - x_iN_0\right] + \frac{(1-p)}{N}\sum_{i=1}^{N}P_t(x^i)\frac{1}{k_i + N_0 + N_1}\left[\sum_{j=1}^{N}A_{ij}|1 - x_i - x_j| + x_iN_1 + (1-x_i)N_0\right] \quad (2)$$

where $k_i = \sum_j A_{ij}$ denotes the degree of the node i. In matrix form this equation becomes $P_{t+1} = UP_t$, where U is the evolution matrix, whose transpose Ω contains the transition probabilities between microstates (Ewens, 2004). In Section 6 we construct Ω explicitly for a ring network with $N=4$.

3. The Moran model with mutations in structured populations

The Moran model describes the evolution of a population of haploid individuals bearing a single gene with alleles 0 and 1. In the original model the dynamics consists in replacing an individual chosen at random by a copy of one of the other individuals, also picked at random. Here we introduce a slightly different version of the dynamics in which an individual is chosen at random and is replaced by its offspring. The offspring is obtained by sexual reproduction between the expiring individual and a mating partner which is also chosen at random among the remaining individuals. The offspring can keep the allele of the expiring individual or that of the mating partner with 50% probability. In the case the offspring keeps the allele of the expiring individual, the population remains unchanged. If it takes the allele from the mating partner, the net effect is that the expiring individual is replaced by a copy of the latter. This alternative dynamics is identical to the Moran process except that it runs twice as slow. The advantage is that we can now introduce mutations during the birth process by allowing the allele received from either parent to change with probability μ_+ from 1 to 0 and μ_- from 0 to 1.

We employ the notation introduced in the previous section for the microscopic state of the population, with x containing information about the haplotype of each individual and x^i representing the state differing from x in the allele of the individual i. Since at each time step only a single individual is replaced, the equation for the probability of finding the population in state x at time $t + 1$, $P_{t+1}(x)$, has a structure similar to Eq. (1):

$$P_{t+1}(x) = \frac{1}{2N}P_t(x)\sum_{i=1}^{N}T(x_i \to x_i) + \sum_{i=1}^{N}\frac{1}{2N}P_t(x^i)T(x_i^i \to x_i). \quad (3)$$

Each of the two terms in Eq. (3) contains two contributions, depending on whether the offspring takes the allele from the expiring individual or from the mating partner. For zero mutation rates the term corresponding to keeping the allele from the expiring individual is analogous to the term $pP_t(x)$ in Eq. (1) (by taking $p = 1/2$). The explicit calculation and simplification of the right-hand side of Eq. (3) is performed in Appendix B. The result reads:

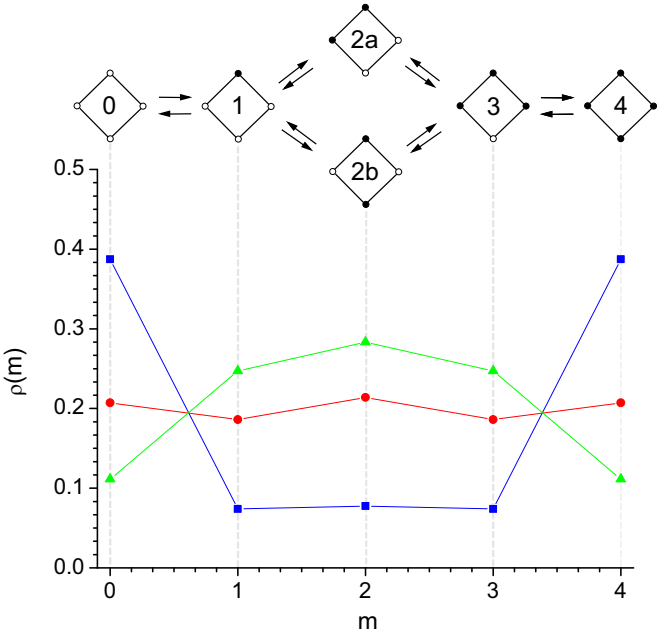

Fig. 1. Top: Microscopic states in the 4 nodes ring and an example of possible transitions. Bottom: Stationary distribution of macroscopic states for $N_0 = N_1 \equiv N_p$; blue squares: N_p=0.1; red circles: N_p=0.579; green triangles: N_p=2.5. The corresponding mutation rates are 0.048, 0.112 and 0.278 respectively.

$$P_{t+1}(x) = P_t(x) + P_t(x)\frac{(1-2\bar{\mu})}{2N}\sum_i \frac{1}{k_i}\Bigg\{\sum_j A_{ij}|1-x_i-x_j| - k_i - \frac{2\mu_+ k_i}{1-2\bar{\mu}}x_i - \frac{2\mu_- k_i}{1-2\bar{\mu}}(1-x_i)\Bigg\} + \frac{(1-2\bar{\mu})}{2N}\sum_i \frac{P_t(x^i)}{k_i}\Bigg\{\sum_j A_{ij}|1-x_i-x_j| + \frac{2k_i\mu_+}{1-2\bar{\mu}}(1-x_i) + \frac{2k_i\mu_-}{1-2\bar{\mu}}x_i\Bigg\} \tag{4}$$

where $\bar{\mu} = (\mu_+ + \mu_-)/2$.

4. Equivalence between the voter and the Moran models

The action of opinion makers in the voter model is not directly equivalent to mutations in the Moran model. In the voter model the copy of an opinion maker does not always correspond to a change of state, since the state of the voter might already be identical to the state of the opinion maker. In the Moran model, on the other hand, a mutation always corresponds to a change of state.

Despite this difference in the dynamical processes, the equations of the voter model can be mapped exactly into the equations of the Moran model for regular networks. To establish this connection we first replace k_i by k in the factors $1/(k_i + N_0 + N_1)$ (in Eq. (2)) and $1/k_i$ (in Eq. (4)). Accordingly, the terms encompassed by the summation symbols in Eqs. (2) and (4) become completely equivalent by identifying

$$\begin{cases} N_1 = \dfrac{2\mu_- k}{1-2\bar{\mu}} \\ N_0 = \dfrac{2\mu_+ k}{1-2\bar{\mu}} \end{cases} \quad \text{or} \quad \begin{cases} \mu_+ = \dfrac{N_0}{N_0+N_1+2k}, \\ \mu_- = \dfrac{N_1}{N_0+N_1+2k}. \end{cases} \tag{5}$$

In turn, the constant pre-factors are related by (see Appendix C)

$$p = \tfrac{1}{2} - \bar{\mu}. \tag{6}$$

The fact that not every action of an opinion maker corresponds to changes in the state of the system is reflected in the fact that the parameter p is mapped to a value that is less than 1/2. Whereas in the Moran Model the offspring keeps the allele of each parent with equal probability and is then subjected to mutation, in the equivalent voter model the voter keeps its opinion with probability $p = 1/2 - \mu < 1/2$ and copies the opinion of a neighbor with probability $1 - p = 1/2 + \mu > 1/2$.

For symmetric processes where $N_0 = N_1 \equiv N_p$ and $\mu_+ = \mu_- \equiv \mu$ Eq. (5) simplifies to

$$N_p = \frac{2\mu k}{1-2\mu} \quad \text{or} \quad \mu = \frac{N_p}{2(N_p+k)}. \tag{7}$$

For non-regular networks it is still possible to establish a map between the two models. This can be accomplished by redefining the intensity of the connection of the node i to the frozen nodes according to its degree k_i:

$$\begin{cases} N_{i1} = \dfrac{2\mu_- k_i}{1-2\bar{\mu}} \\ N_{i0} = \dfrac{2\mu_+ k_i}{1-2\bar{\mu}} \end{cases} \quad \text{or} \quad \begin{cases} \mu_+ = \dfrac{N_{i0}}{N_{i0}+N_{i1}+2k_i} \\ \mu_- = \dfrac{N_{i1}}{N_{i0}+N_{i1}+2k_i}. \end{cases} \tag{8}$$

In this case the perturbation caused by the frozen nodes can be interpreted as acting on the links of the free nodes, so that the more links a node has, the stronger the perturbation it experiences. This modification does not alter the form of relation (6).

5. Phase transition in fully connected networks

Fully connected networks correspond to panmictic populations in the Moran model. In this case the dynamics of the voter model can be solved analytically (Chinellato et al., 2015). For $N_0 = N_1 \equiv N_p$ the probability of finding the network with m nodes in state 1 is given by the Beta-Binomial distribution

$$\rho_{FC}(m) = \mathcal{A}(N, N_p)\frac{(N_p+m-1)!(N+N_p-m-1)!}{(N-m)!m!}, \tag{9}$$

where $\mathcal{A}(N, N_p)$ is a normalization factor. Defining $x_m = m/N$ and taking the limit $N \to \infty$, x_m becomes a continuous variable $0 \le x \le 1$ and ρ converges to the Beta distribution (Kirman, 1993; Gillespie, 2004)

$$\rho_{FC}(x) = \frac{\Gamma(2N_p)}{\Gamma(N_p)^2}\left[x(1-x)\right]^{N_p-1}. \tag{10}$$

The system displays a phase transition at $N_p = 1$. For $N_p > 1$ the network is in a disordered state where, on the average, half the nodes are in state 1 and half in state 0. The distribution is Gaussian shaped and its variance narrows as N_p increases. For $N_p < 1$ most nodes are in state 0 or in state 1, describing an ordered scenario with a U-shaped distribution (Crow and Kimura, 1970; Gillespie, 2004). At the phase transition $N_p \equiv N_c = 1$ any number of nodes can be found in state 1 (or 0) with equal probability.

According to Eq. (7) a transition occurs in the Moran model at $\mu \equiv \mu_c = 1/2N$ (Gillespie, 2004). The ordered states of the network represent near fixation of one of the alleles, whereas the disordered state corresponds to a random distribution of alleles in the population. In the following sections we study the phase transition for non-fully connected regular networks ($k < N-1$).

6. Example: a ring network with 4 nodes

For small regular networks the transition probabilities can be calculated explicitly. Here we illustrate the calculation in the context of the voter model for a ring network with four nodes.

According to Fig. 1, the transition matrix Ω can be written as

$$\Omega = \frac{1}{4(2+N_0+N_1)}W, \tag{11}$$

where W is given by

$$W = \begin{array}{c|ccccccc} \text{state} & 0 & 1 & 2a & 2b & 3 & 4 \\ 0 & 4(2+N_0) & 4N_1 & 0 & 0 & 0 & 0 \\ 1 & N_0+2 & N_1+3N_0+4 & 2(1+N_1) & N_1 & 0 & 0 \\ 2a & 0 & 2(1+N_0) & 2(2+N_0+N_1) & 0 & 2(1+N_1) & 0 \\ 2b & 0 & 2(2+N_0) & 0 & 2(N_0+N_1) & 2(2+N_1) & 0 \\ 3 & 0 & 0 & 2(1+N_0) & N_0 & N_0+3N_1+4 & N_1+2 \\ 4 & 0 & 0 & 0 & 0 & 4N_0 & 4(2+N_1) \end{array}$$

The evolution matrix U, corresponding to the transpose of Ω, has one eigenvalue $\lambda = 1$. This eigenvector describes the stationary state, and it has components

$$v_0 = N_0(2+N_0)\left[2(4+N_1)+N_0(22+6N_1+N_0(16+3N_0+3N_1))\right]$$
$$v_1 = 4N_0N_1[2(4+N_1)+N_0(22+6N_1+N_0(16+3N_0+3N_1))]$$
$$v_{2a} = 4N_0N_1\left[8+3N_0^2(1+N_1)+3N_1(4+N_1)+N_0(12+N_1(16+3N_1))\right]$$
$$v_{2b} = 2N_0N_1[2N_1+N_0(2+N_1(10+3N_0+3N_1))]$$
$$v_3 = 4N_0N_1[N_0(2+3N_1(2+N_1))+(4+3N_1)(2+N_1(4+N_1))]$$
$$v_4 = N_1(2+N_1)\left[N_0(2+3N_1(2+N_1))+(4+3N_1)(2+N_1(4+N_1))\right]$$

The stationary probability distribution of the macroscopic states σ_m is computed as:

$$\rho(0) = av_0$$
$$\rho(1) = av_1$$
$$\rho(2) = a(v_{2a}+v_{2b})$$
$$\rho(3) = av_3$$
$$\rho(4) = av_4$$

where $a^{-1} = v_0+v_1+v_{2a}+v_{2b}+v_3+v_4$.

Fig. 1 shows the stationary distribution of macroscopic states at equilibrium for $N_0 = N_1 = N_p$ with N_p=0.1 (blue), N_p=0.579 (red) and N_p=2.5 (green). Note that, contrary to the full connected case, the transition between disordered states (green) and ordered states (blue) does not go through the flat curve $\rho(m) = \frac{1}{N+1} = 1/5$, but displays a small amplitude oscillation around this value. For our purpose, we define the critical point in this case to be the value of N_p for which $\rho(4) = \rho(0)$ becomes equal to $\rho(2)$. The corresponding value can be obtained analytically, and corresponds to $N_p = 2/5(\sqrt{6}-1) \approx 0.579$.

7. Phase transitions in regular networks

In this section we show numerical simulations for regular networks of size N where each node is connected to an even number k of nearest neighbors (see Fig. 2). Specifically, we focus in the transition between ordered and disordered states for $k < N-1$. We use the framework of the voter model, where approximate expressions are available for general networks, and symmetric perturbations $N_0 = N_1 \equiv N_p$. We then translate the results to mutation rates using Eq. (7).

It was shown in de Aguiar et al. (2009) that for general networks the equilibrium distribution can be approximated by

$$\rho(m, N_p) = \rho_{FC}\left(m, \frac{N_p(N-1)}{\langle k\rangle}\right), \tag{12}$$

where we have indicated explicitly the value N_p of the perturbation and $\langle k\rangle$ is the average degree of the network. In this approximation the critical perturbation is given by $\tilde{N}_c = \langle k\rangle/(N-1)$. Using Eq. (7) we find that $\mu_c = 1/2N$, independent of $\langle k\rangle$. Therefore, in a first approximation, the genetic equilibrium distribution of a Moran process is insensitive to the population spatial structure. We show below that this approximation fails for small $\langle k\rangle$.

Our results correspond to simulations for macroscopic states σ_m, defined as the configuration where $0 \le m \le N$ nodes are in the state 1. We plot the probability $\rho(m)$ of finding the network in state σ_m at equilibrium (Fig. 3). We find that the behavior obtained analytically for N=4 holds in the general case: for large N_p the distribution is Gaussian shaped and peaked at $N/2$. As N_p decreases the distribution becomes flat only if $k = N-1$, given by $\rho(m) = 1/(N+1)$. For $k < N-1$ the probabilities $\rho(0)$ and $\rho(N)$ increase faster than that of their neighbor macroscopic states and become larger than $1/(N+1)$ before the center of the distribution flattens out. Therefore, the transition is smooth, and no true critical point exists. In order to compare the results of structured populations with the panmictic case, we define, as in the previous section, the transition point N_c as the value of N_p where $\rho(0) = \rho(N)$ becomes equal to $\rho(N/2)$.

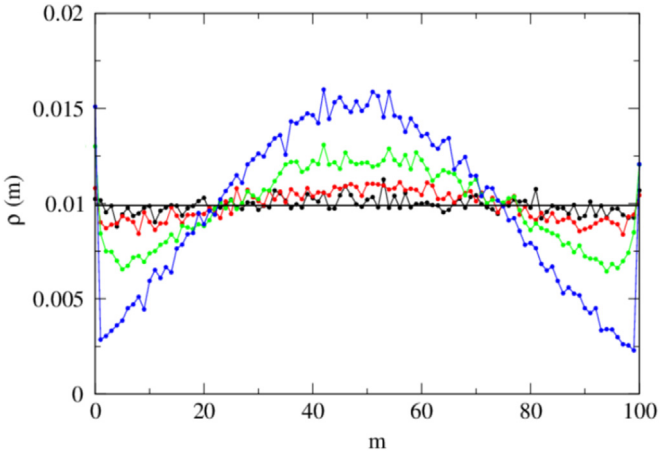

Fig. 3. Macroscopic probability distribution at equilibrium and critical point for ring networks with N=100 and degrees k=30 (black squares), 20 (red circles), 10 (green triangles) and 2 (blue stars). The thick black line shows the flat distribution obtained analytically for fully connected networks, $k = N-1$. The distributions correspond to 10^4 realizations of the dynamics.

Fig. 3 shows the distribution $\rho(m)$ at the transition point for a regular network with N=100 and several values of k. For large k, $\rho(m)$ is close to the flat distribution displayed by fully connected networks with N_c very close to $\tilde{N}_c = k/(N-1)$, as predicted in de Aguiar et al. (2009), but for small k it differs significantly. The transition from Gaussian like to U-shaped distribution goes through a trimodal phase with peaks at m=0, $m = N/2$ and m=N. The value of N_c is also consistently smaller than $\tilde{N}_c$.

We have calculated N_c numerically for several values of k for N=20, 30, 50, 100, 200, 250, 300 and 350. For each value of N we compared the result with the approximation $\tilde{N}_c$ computing the ratio

$$f(N,k) \equiv \frac{\tilde{N}_c}{N_c}. \tag{13}$$

Using these numerical values we obtained the power-law fit

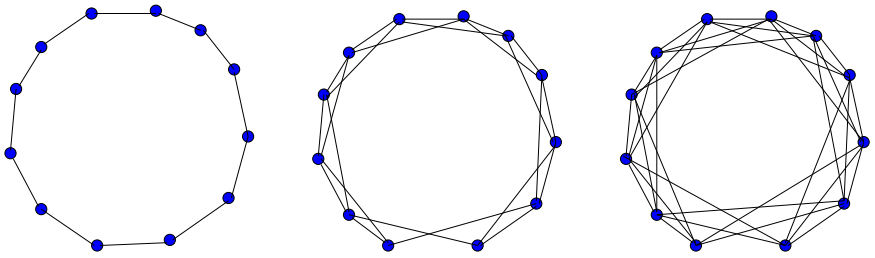

Fig. 2. Regular networks with degrees k=2, 4 and 6.

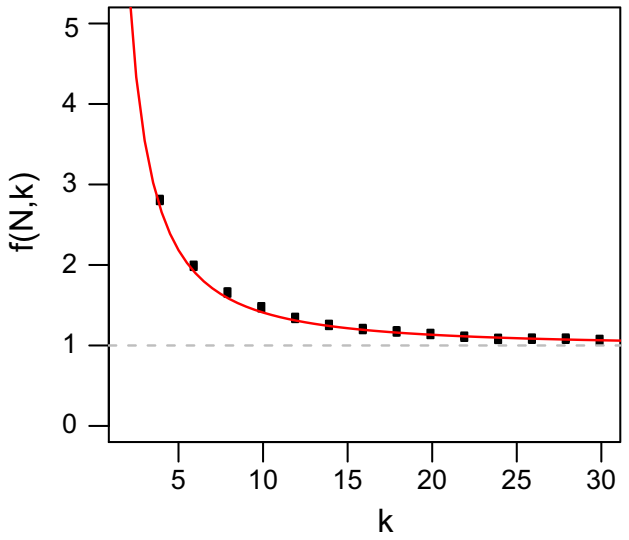

Fig. 4. Ratio between $\tilde{N}_c = k/(N-1)$ and numerically computed values of N_c (black squares connected by lines) for $N=100$. The red curve shows the numerical fit using Eq. (14).

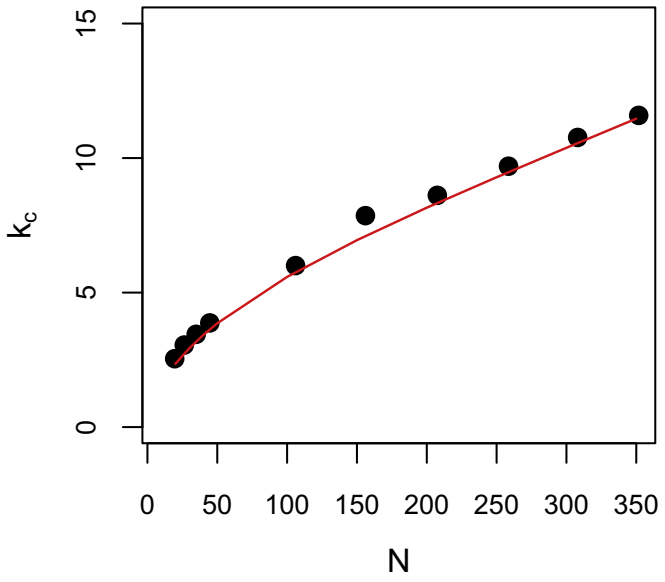

Fig. 5. Critical degree k_c as a function of N. The dots show the results calculated directly from setting the numerically computed $f(N, k)$ to 2 and the line is Eq. (17).

$$f(N, k) = 1 + A(N - k + 1)k^{-k_0} \tag{14}$$

where $k_0 = 1.457 \pm 0.007$. The amplitude $A = A(N)$ depends weakly on N as $A(N) = a_0 + a_1 N + a_2 N^{a_3}$, with $a_0 = -3.69 \pm 0.02$, $a_1 = 0.00012 \pm 0.00005$, $a_2 = 4.0 \pm 0.2$ and $a_3 = -0.016 \pm 0.004$. The fitted curve and the numerical results are illustrated in Fig. 4 for $N=100$.

Substituting Eqs. (13) and (14) in (5) with $N_0 = N_1 = N_c$ and $\mu_+ = \mu_- = \mu_c$, we can calculate the analogous critical mutation rate above which fixation of either allele is unlikely. The result is

$$\mu_c(N, k) = \frac{1}{2[1 + (N-1)f(N, k)]}. \tag{15}$$

The ratio between the panmictic critical mutation $\mu_{cp} = 1/2N$ and the actual value $\mu_c(N, k)$ is

$$\frac{\mu_{cp}}{\mu_c(N, k)} = \frac{2 + 2(N-1)f(N, k)}{2N} \approx f(N, k) \tag{16}$$

for large N.

In order to have a measure of how much spatial structure is necessary to significantly affect the genetic distribution we define k_c as the degree where the critical mutation drops to half of its panmictic value, which, according to Eq. (16), is equivalent to set $f(N, k_c) = 2$. Using Eqs. (14)–(15) we obtain, in the limit of large N,

$$k_c(N) = \left[NA(N)\right]^{1/k_0}. \tag{17}$$

The accuracy of this formula is shown in Fig. 5.

Fig. 6 illustrates the behavior of μ_c as a function of k for a larger population with $N=10{,}000$ using Eqs. (15) and (14). The critical mutation stays close to $1/2N$ for $k > 2000$. For $k = k_c \approx 640$ μ_c decreases to half of its panmictic value and for $k \approx 150$ to a tenth of it. For $k \approx 20$ μ_c drops to 1% of its panmictic value.

The connectivity needed for a substantially smaller value of the critical mutation rate is small and grows slowly with the population size, indicating that isolation by distance requires high degrees of spatial structure, as suggested by numerical simulations using individual based models (de Aguiar et al., 2009; Martins et al., 2013). As shown in Fig. 6, diversity can be increased either by increasing the mutation rate at fixed k or by decreasing k at fixed mutation rate.

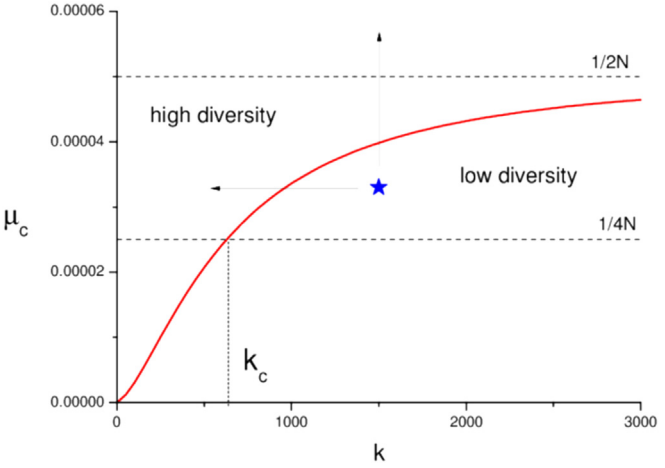

Fig. 6. Mutation threshold $\mu_c(N, k)$ for $N=10000$. For a given a connectivity and mutation rate (blue star) the genetic diversity of the population can increase by either increasing the mutation rate (vertical arrow) or decreasing the connectivity (horizontal arrow).

8. Discussion

The dynamics of allele frequencies in spatially structured populations is a key element for understanding evolution and has been part of theoretical population genetics from its beginning (Gillespie, 2004). In addition, incorporating spatial structure in evolutionary models is part of the goal of making models more realistic, allowing for a better description of natural populations (Hey and Machado, 2003). Recently, evolutionary graph theory has been suggested as a new approach to study the effect of population structure on evolution (Nowak, 2006). However, it is still not clear to what extent the results obtained within this framework are comparable to other models that have been vastly explored in the literature (*e.g.* island or stepping-stone models).

So far, models relying on evolutionary graph theory (Lieberman et al., 2005; Whigham and Dick, 2005; Voorhees, 2013; Allen, 2015) have usually yielded qualitatively similar results when compared to those known from other approaches (Nagylaki, 1980; Whitlock and Barton, 1997; Whitlock, 2003) and reviewed in

Ewens (2004) and Gillespie (2004). For beneficial or deleterious alleles, spatial structure is known to affect evolutionary dynamics. It can, for example, increase or decrease fixation probability depending on spatial topology (Whitlock, 2003; Lieberman et al., 2005; Voorhees, 2013). On the other hand, for neutral loci spatial structure is thought to be less important. While it is known to affect the time to fixation (Ewens, 2004; Whigham and Dick, 2005), fixation probabilities are expected to remain unchanged (Ewens, 2004). Very low migration rates are required for the effect of population subdivision to substantially affect the maintenance of neutral variability (reviewed in Ewens, 2004), and its consequences are often summarized by the calculation of an effective population size in relation to some specific property of the problem in question (*e.g.* Wright's Fst; Ewens, 2004; Gillespie, 2004; Charlesworth, 2009). Spatial variation in additional properties of the model can increase the effect of spatial structure on the dynamics of neutral alleles. Using a Wright–Fisher type demic model, Nagylaki (1980) has shown that spatially structured populations displayed the same behavior as well-mixed ones if migration is relatively strong, and only if it is symmetric and does not alter deme size. However, drift can have increased importance in the neutral dynamics of structured populations if there is spatial variation in birth or death rate (Allen, 2015) or among deme variation in immigration and emigration rates, extinction and colonization (Whitlock and Barton, 1997).

In this work, we considered a single biallelic gene in a population evolving under the Moran dynamics and distributed on a regular network, where every node has the same k number of neighbors. This arrangement is an idealized representation of a population's spatial structure and models restrictions in gene flow promoted by spatial distance. For $k = N - 1$ the network is fully connected, representing a well-mixed population. The other extreme, $k=2$, corresponds to a ring and describes a sparsely connected population, distributed, for example, along the shore of an island. Networks with $2 < k < N - 1$ interpolate between these two cases and allow the study of the effects of gradually decreasing the amount of spatial structuring. Adopting the graph theory approach allowed us to use an approximate solution known for the closely related voter model. While previous models have focused on the effect of population structure on fixation probabilities or effective population size, we turned our attention to the equilibrium distributions under the mutation–drift balance. We show that spatial structure affects the shift in regimes observed in the equilibrium distributions of allele frequencies, allowing lower mutation rates to dominate over drift. In consonance with classical results, extreme restriction in gene flow is required for structuring to have an effect. In fact, the critical mutation rate above which drift is overcome changes significantly only when the degree of the network becomes very small, $k \lesssim k_c$.

However, in contrast to other models in the literature, we found that the transition between these regimes is qualitatively different from that observed in well-mixed populations. The shape of the allele distribution $\rho(m)$ at the transition $\mu = \mu_c$ has a curious trimodal structure with a central broad peak at $m = N/2$ and two narrow peaks at $m=0$ and $m=N$. In well-mixed populations, the equilibrium allele distribution converges to a Beta distribution which is equal to a standard uniform distribution at this transition (both shape parameters equal to 1). To our knowledge, this is the only case reported where the dynamics of structured populations differs qualitatively from well-mixed populations.

If so, the role of mutation on diversity could be underestimated and the interaction of new mutations occurring on the same site and mutation reversion could be more important than we currently think. In well-mixed populations, mutation is expected to dominate over drift when $4N\mu > 1$ for diploid populations or $2N\mu > 1$ for haploid populations and much higher genetic diversity is expected under neutrality. Estimates from nucleotide diversity suggest that $N_e\mu$ is, typically, less than 0.024 for unicellular and less than 0.008 for multicellular eukaryotes (Lynch and Conery, 2003) and N_e is expected to be several orders of magnitude smaller than $1/\mu$. For all one knows, this is maybe the reason why this transition in the mutation–drift balance has been less explored when compared to other aspects of population genetics theory. In our numerical simulations the degree of the network for which the mutation threshold drops to half of its panmictic value was found to depend on N^{1/k_0}, with k_0 close to 1.5 (Eq. (17)). The parameter k_0 was estimated from simulations with $N \leq 350$. Simulations for larger values of N would be required to better estimate this parameter, however, the computational costs are prohibitive at this point. Despite this limitation, it is already clear that the sensitivity of the allele composition of the population to the spatial structure requires an important reduction in the number of potential mating partners of a given individual. However, at least for vertebrate species, the number of potential partners accessed by an individual may be surprisingly small. The number of males surveyed by a female for 20 vertebrate species was found to be less than 20 (mean = 4.5, median = 2.9) (Roff and Fairbairn, 2014). Although these values are not directly comparable to the degree of the network in our model, they can give some insight on how the variables are expected to scale in real case scenarios. From our results (Fig. 6), the critical mutation, μ_c, approaches zero as the number of potential partners decreases. For example, if $k < 20$, mutation dominates over drift when $N\mu \gtrsim 0.005$.

It is interesting to note that the effect of population structure in enhancing the effective mutation rate would also apply to migrations from an external source. If migrants with allele 0 or 1 arrive with equal probability and replace residents at random locations, their effect would be similarly enhanced by the local spatial structure.

For organisms with asexual reproduction, our models have an alternative interpretation relating to random variation in the number of descendants. Estimates of $N_e\mu$ are considerably higher for prokaryotes. While it is well-recognized that the microbial populations are spatially structured (Martiny et al., 2006), they are not expected to be as structured as required for the effect seen in our model to be relevant. In this context, however, it is worth mentioning that transition between the two regimes in the mutation–drift balance defines a critical mutation similar to the mutation threshold leading to the error catastrophe due to the balance between mutation and frequency-independent (Eigen, 1971) or frequency-dependent selection (de Aguiar et al., 2015) in the Eigen model.

Acknowledgments

We thank Yaneer Bar-Yam and two anonymous reviewers for helpful suggestions on the manuscript. M.A.M.A. and A.B.M acknowledge financial support from São Paulo Research Foundation (FAPESP), grants #2014/04036–2 and #2014/10470–7. M.A.M.A. and D.M.S. acknowledge financial support from CNPq.

Appendix A. Dynamics in the voter model

According to the dynamical rules the transition probabilities can be written as:

$$T(x_i \to x_i) = \frac{1}{k_i + N_0 + N_1}\left[\sum_{j=1}^{N} A_{ij}|1 - x_i - x_j| + x_i N_1 + (1 - x_i)N_0\right] \quad \text{(A1)}$$

where k_i is the degree of node i. This is the sum over all connected neighbors identical in state with i divided by the total number of neighbors. Similarly

$$T(x_i^i \to x_i) = \frac{1}{k_i + N_0 + N_1}\left[\sum_{j=1}^{N} A_{ij}|x_i^i - x_j| + (1 - x_i^i)N_1 + x_i^i N_0\right]. \quad \text{(A2)}$$

Using $x_i^i = 1 - x_i$ we find that the two transition probabilities are identical. However, instead of putting them together we write $pP_t(x)$ as $P_t(x) - (1 - p)P_t(x)$ to obtain

$$\begin{aligned} P_{t+1}(x) = {} & P_t(x) + \frac{(1-p)}{N}P_t(x)\sum_{i=1}^{N}\frac{1}{k_i + N_0 + N_1}\left[\sum_{j=1}^{N} A_{ij}|1 - x_i - x_j|\right. \\ & \left. - k_i - (1 - x_i)N_1 - x_i N_0\right] \\ & + \frac{(1-p)}{N}\sum_{i=1}^{N} P_t(x^i)\frac{1}{k_i + N_0 + N_1}\left[\sum_{j=1}^{N} A_{ij}|1 - x_i - x_j|\right. \\ & \left. + x_i N_1 + (1 - x_i)N_0\right]. \end{aligned} \quad \text{(A3)}$$

Appendix B. Dynamics in the Moran model

The contributions to $P_{t+1}(x)$ in Eq. (3) can be divided into four terms, so that

$$P_{t+1}(x) = P_1 + P_2 + P_3 + P_4. \quad \text{(B1)}$$

The first two are related to the transition $T(x_i \to x_i)$ describing the situations where

P_1: the previous state of the population is x and the offspring gets the allele from the expiring individual;

P_2: the previous state is x and the offspring gets the allele from the other parent.

The other terms refer to the transition $T(x_i^i \to x_i)$ when

P_3: the previous state is x^i, i is chosen to be replaced and the offspring gets the allele from the expiring individual.

P_4: the previous state is x^i, i is chosen to be replaced and the offspring gets the allele from the other parent.

Calculation of P_1: Here we need to consider the probability of picking individual i $(1/N)$ times the probability that the offspring takes its allele $(1/2)$ and sum over all individuals. If $x_i=1$ it should not mutate to 0 and if $x_i=0$ it should not mutate to 1. We obtain

$$\begin{aligned} P_1 &= P_t(x)\sum_i \frac{1}{2N}[x_i(1 - \mu_+) + (1 - x_i)(1 - \mu_-)] \\ &= P_t(x)\frac{1}{2N}\sum_i [1 - x_i\mu_+ - (1 - x_i)\mu_-] \\ &= P_t(x) - \frac{1}{2N}\sum_i [1 + x_i\mu_+ + (1 - x_i)\mu_-] \end{aligned} \quad \text{(B2)}$$

Calculation of P_2: Here the offspring gets the allele of a connected individual, which can have the same allele as the focal individual or the opposite allele.

$$\begin{aligned} P_2 &= P_t(x)\frac{1}{2N}\sum_i \frac{1}{k_i}\left\{\sum_j A_{ij}|1 - x_i - x_j|\right. \\ &\quad \left.[x_i(1 - \mu_+) + (1 - x_i)(1 - \mu_-)] + \sum_j A_{ij}|x_i - x_j|\right. \\ &\quad \left.[x_i\mu_- + (1 - x_i)\mu_+]\right\} \\ &= P_t(x)\frac{1}{2N}\sum_i \frac{1}{k_i}\left\{\sum_j A_{ij}|1 - x_i - x_j|\right. \\ &\quad \left.[x_i(1 - 2\bar{\mu}) + (1 - x_i)(1 - 2\bar{\mu})]\right. \\ &\quad \left. + \sum_j A_{ij}[x_i\mu_- + (1 - x_i)\mu_+]\right\} \\ &= \frac{P_t(x)}{2N}\sum_i \frac{1}{k_i}\left\{\sum_j A_{ij}|1 - x_i - x_j|\right. \\ &\quad \left.(1 - 2\bar{\mu}) + k_i[x_i\mu_- + (1 - x_i)\mu_+]\right\} \end{aligned} \quad \text{(B3)}$$

From the first to second line we used that $|x_i - x_j| = 1 - |1 - x_i - x_j|$ and re-arranged the terms. We have also defined

$$\bar{\mu} = (\mu_+ + \mu_-)/2. \quad \text{(B4)}$$

and used $\sum_j A_{ij} = k_i$.

Adding P_1 and P_2: The terms without the adjacency matrix in P_2 add to those in P_1. If we factor out $(1 - 2\bar{\mu})$ we get

$$\begin{aligned} P_1 + P_2 = P_t(x) + P_t(x)\frac{1 - 2\bar{\mu}}{2N}\sum_i \frac{1}{k_i}\left\{\sum_j A_{ij}|1 - x_i - x_j|\right. \\ \left.[\frac{(1 - 2x_i)\mu_+ k_i}{1 - 2\bar{\mu}} - \frac{(1 - 2x_i)\mu_- k_i}{1 - 2\bar{\mu}} - \frac{k_i}{1 - 2\bar{\mu}}]\right\}. \end{aligned} \quad \text{(B5)}$$

In order to compare with the network model we change the last term as follows:

$$\frac{k_i}{1 - 2\bar{\mu}} = k_i + \frac{2\bar{\mu}k_i}{1 - 2\bar{\mu}} = k_i + \frac{\mu_+ k_i}{1 - 2\bar{\mu}} + \frac{\mu_- k_i}{1 - 2\bar{\mu}}$$

Substituting above we get

$$\begin{aligned} P_1 + P_2 = P_t(x) + P_t(x)\frac{1 - 2\bar{\mu}}{2N}\sum_i \frac{1}{k_i}\left\{\sum_j A_{ij}|1 - x_i - x_j|\right. \\ \left. - k_i - \frac{2\mu_+ k_i}{1 - 2\bar{\mu}}x_i - \frac{2\mu_- k_i}{1 - 2\bar{\mu}}(1 - x_i)\right\}. \end{aligned} \quad \text{(B6)}$$

Compare with the first and second lines of Eq. (2) and we can see the similarity already.

Calculation of P_3: Here the previous state of the population is x^i and it differs from x by individual i, which has the opposite allele. For the state x^i to change to x the offspring must inherit the allele from i and mutate. The probability of picking that particular individual i is $(1/N)$ and we must sum over all possible states x^i. The probability that the offspring takes its allele is 1/2 and, in that case, it must mutate to change the allele.

$$P_3 = \sum_i P_t(x^i)\frac{1}{2N}[x_i^i\,\mu_+ + (1 - x_i^i)\mu_-] \quad \text{(B7)}$$

Calculation of P_4: The situation is similar to P_3, but the offspring gets the allele of a connected individual with allele different from x_i^i:

$$P_4 = \frac{1}{2N}\sum_i P_t(x^i)\frac{1}{k_i}\Bigg\{\sum_j A_{ij}|x_i^i - x_j| \\ [x_i^i(1-\mu_-) + (1-x_i^i)(1-\mu_+)] + \sum_j A_{ij}|1 - x_i^i - x_j| \\ [x_i^i\mu_+ + (1-x_i^i)\mu_-]\Bigg\} \\ = \frac{1}{2N}\sum_i \frac{P_t(x^i)}{k_i}\Bigg\{\sum_j A_{ij}|1 - x_i - x_j| \\ [(1-x_i)(1-2\bar{\mu}) + x_i(1-2\bar{\mu})] + k_i[(1-x_i)\mu_+ + x_i\mu_-]\Bigg\} \quad \text{(B8)}$$

where we used that $x_i^i = 1 - x_i$ and that $|x_i - x_j| = 1 - |1 - x_i - x_j|$. Adding P_3 and P_4 amounts to factors of 2 in the terms in the last line. Factoring out $1 - 2\bar{\mu}$, we get

$$P_3 + P_4 = \frac{1-2\bar{\mu}}{2N}\sum_i \frac{P_t(x^i)}{k_i}\Bigg\{\sum_j A_{ij}|1 - x_i - x_j| \\ + \frac{2k_i\mu_+}{1-2\bar{\mu}}(1-x_i) + \frac{2k_i\mu_-}{1-2\bar{\mu}}x_i\Bigg\} \quad \text{(B9)}$$

The final result is

$$P_{t+1}(x) = P_t(x) + P_t(x)\frac{(1-2\bar{\mu})}{2N}\sum_i \frac{1}{k_i}\Bigg\{\sum_j A_{ij}|1 - x_i - x_j| \\ - k_i - \frac{2\mu_+k_i}{1-2\bar{\mu}}x_i - \frac{2\mu_-k_i}{1-2\bar{\mu}}(1-x_i)\Bigg\} \\ \frac{(1-2\bar{\mu})}{2N}\sum_i \frac{P_t(x^i)}{k_i}\Bigg\{\sum_j A_{ij}|1 - x_i - x_j| \\ + \frac{2k_i\mu_+}{1-2\bar{\mu}}(1-x_i) + \frac{2k_i\mu_-}{1-2\bar{\mu}}x_i\Bigg\} \quad \text{(B10)}$$

Appendix C. Rates of mutation in the Moran and voter models

The connection between the voter and Moran models in regular networks requires that the number of opinion makers and the mutation rates have to be related by Eq. (5). In order for the master equations to be completely equivalent we also need to identify

$$\frac{1-p}{N(k+N_0+N_1)} \equiv \frac{1-2\bar{\mu}}{2Nk} \quad \text{(C1)}$$

or

$$2k(1-p) = (1-2\bar{\mu})(k+N_0+N_1). \quad \text{(C2)}$$

Using Eq. (5) we obtain

$$N_0 + N_1 = \frac{4k\bar{\mu}}{1-2\bar{\mu}}$$

or

$$(1-2\bar{\mu})(N_0+N_1) = 4k\bar{\mu}.$$

Substituting this expression in (C2) we obtain

$$2k(1-p) = (1-2\bar{\mu})k + 4k\bar{\mu} = (1+2\bar{\mu})k.$$

Canceling k on both sides and rearranging the terms we obtain $p = 1/2 - \bar{\mu}$.

References

Allen, B., Sample, C., Dementieva, Y., Medeiros, R.C., Paoletti, C., Nowak, M.A., 2015. PLoS Comput. Biol. 11. http://dx.doi.org/10.1371/journal.pcbi.1004108.
Cannings, C., 1974. Adv. Appl. Probab. 6, 260.
Charlesworth, B., 2009. Nat. Rev. Genet. 10, 195.
Chinellato, D.D., Epstein, I.R., Braha, D., Bar-Yam, Y., Aguiar, M.A.M.d., 2015. J. Stat. Phys. 159, 221.
Constable, G.W.A., McKane, A.J., 2014. J. Theoret. Biol. 358, 149.
Crow, J.F., Kimura, M., 1970. An Introduction to Population Genetics Theory. The Blackburn Press, Caldwell, NJ, USA.
Débarre, F., Hauert, C., Doebeli, M., 2014. Nat. Commun. 5. http://dx.doi.org/10.1038/ncomms4409.
de Aguiar, M.A.M., Bar-Yam, Y., 2011. Phys. Rev. E 84, 031901.
de Aguiar, M.A.M., Baranger, M., Baptestini, E.M., Kaufman, L., Bar-Yam, Y., 2009. Nature 460, 384.
de Aguiar, M.A.M., Schneider, D.M., do Carmo, E., Campos, P.R.A., Martins, A.B., 2015. J. Theor. Biol. 374, 48.
Dick, G., Whigham, P., 2005. The 2005 IEEE Congress on Evolutionary Computation, 2005, Vol. 2. pp. 1855–1860.
Durrett, R., Moseley, S., 2015. Ann. Appl. Probab. 25, 104.
Eigen, M., 1971. Naturwissenschaften 58, 465.
Ewens, W.J., 2004. Mathematical Population Genetics 1: Theoretical Introduction, 2nd ed. Springer, New York.
Gillespie, J., 2004. Population Genetics: A Concise Guide, 2nd ed. Johns Hopkins University Press, Baltimore, MD.
Gladstien, K., 1978. SIAM J. Appl. Math. 34, 630.
Gordo, I., Campos, P.R.A., 2006. Genetica 127, 217.
Harmon, D., Lagi, M., de Aguiar, M.A.M., Chinellato, D.D., Braha, D., Epstein, I.R., Bar-Yam, Y., 2015. PLoS ONE 10, e0131871.
Hey, J., Machado, C.A., 2003. Nat. Rev. Genet. 4, 535.
Kirman, A., 1993. Quart. J. Econ. 108, 137.
Lenormand, T., Roze, D., Rousset, F., 2009. Trends Ecol. Evol. 24 (157).
Lieberman, E., Hauert, C., Nowak, M.A., 2005. Nature 433, 312.
Liggett, T., 2012. Interacting Particle Systems. Springer Science & Business Media.
Lynch, M., Conery, J.S., 2003. Science 302, 1401.
Martins, A.B., Aguiar, M.A.M.d., Bar-Yam, Y., 2013. Proc. Natl. Acad. Sci. U.S.A. 110, 5080.
Martiny, J.B.H., Bohannan, B.J.M., Brown, J.H., Colwell, R.K., Fuhrman, J.A., Green, J.L., Horner-Devine, M.C., Kane, M., Krumins, J.A., Kuske, C.R., Morin, P.J., Naeem, S., Vres, L., Reysenbach, A.-L., Smith, V.H., Staley, J.T., 2006. Nat. Rev. Microbiol. 4, 102.
Mobilia, M., Petersen, A., Redner, S., 2007. J. Stat. Mech. Theory Exp. P08029.
Mobilia, M., 2003. Phys. Rev. Lett. 91, 028701.
Monk, T., Green, P., Paulin, M., 2014. Proc. R. Soc. A 470, 20130730.
Nagylaki, T., 1980. J. Math. Biol. 9, 101.
Nowak, M.A., 2006. Evolutionary Dynamics: Exploring the Equations of Life, first edition. Belknap Press, Cambridge, Mass.
Patwa, Z., Wahl, L.M., 2008. J. R. Soc. Interface 5, 1279.
Roff, D.A., Fairbairn, D.J., 2014. Ecol. Evol. 4, 2759.
Tarnita, C.E., Antal, T., Nowak, M.A., 2009. J. Theor. Biol. 261, 50.
Voorhees, B., 2013. Proc. R. Soc. London A: Math. Phys. Eng. Sci. 469, 20120248.
Watterson, G.A., 1961. Ann. Math. Stat. 32, 716.
Whigham, P.A., Dick, G., 2005. Fixation of neutral alleles in spatially structured populations via genetic drift: describing the spatial structure of faster-than-panmictic configurations, pp. 81–90, Presented at the 17th Annual Colloquium of the Spatial Information Research Centre (SIRC 2005: A Spatio-temporal Workshop), http://hdl.handle.net/10523/685.
Whigham, P.A., Dick, G. 2007. Genet. Program. Evol. Mach. 9, 157.
Whitlock, M.C., Barton, N.H., 1997. Genetics 146, 427.
Whitlock, M.C., 2003. Genetics 164, 767.
Wright, S., 1931. Genetics 16, 97.
Yildiz, E., Ozdaglar, A., Acemoglu, D., Saberi, A., Scaglione, A., 2013. ACM Trans. Econ. Comput 1 (19), 1.